Nonparaxial solitary waves in anisotropic dielectrics

Alessandro Alberucci* and Gaetano Assanto†

Nonlinear Optics and OptoElectronics Lab (NooEL), University 'Roma Tre', Via della Vasca Navale 84, IT-00146 Rome, Italy

(Received 4 May 2010; published 21 March 2011)

We account for the vectorial character of electromagnetic waves in the study of nonlinear self-action and transverse localization in dielectric anisotropic media. With reference to uniaxials, we address spatial solitons propagating in the nonparaxial regime in the presence of an arbitrary degree of nonlocality, going from the standard Kerr response to the highly nonlocal case, unveiling various effects, including transverse profile asymmetry and bending of the trajectory, as well as a weak effective nonlocality even in local media.

DOI: 10.1103/PhysRevA.83.033822 PACS number(s): 42.65.Jx, 05.45.Yv, 42.65.Tg

I. INTRODUCTION

Nonlinear self-action and wave self-localization in solitary or singular forms have received substantial attention in the fields of fluid dynamics, plasmas, Bose-Einstein condensates, acoustics, biology, soft matter, and optics [1–6]. Particularly in optics, a revival of interest was brought about by considering nonlocality in media supporting two-dimensional solitary waves, whereby nonlocal or "accessible" solitons are stable in propagation and robust against perturbations [7–11]. In most materials, however, the nonlinear mechanism yielding self-action and beam self-trapping is associated with anisotropy, since it depends on the polarization of the wave and on its direction of propagation. The latter applies, e.g., to semiconductor and liquid crystals, quadratic as well as Kerr-like dielectrics [11–20]. High nonlinearities can also result in wavelength-scale light confinement, making nonparaxiality relevant [21]. From Lax's pioneering work on nonparaxial waves [22], several models of nonparaxial nonlinear propagation have been developed [23–28]. Exact solutions of Maxwell's equations were found in Ref. [29] in the form of self-confined nonparaxial dark solitons with an azimuthal polarization. Tight electromagnetic confinement in subwavelength structures has become important in the rapidly growing field of plasmonics [30–32], as well as in the context of optical tweezers [33,34] and nanostructured fibers [35].

In this paper we study electromagnetic self-trapping in uniaxials, in the presence of arbitrarily large nonlinearity and nonlocality. Starting from Maxwell's equations we model nonparaxial spatial solitons in geometries where ordinary and extraordinary field components are decoupled and predict the insurgence of asymmetry in their transverse profile and bending of their propagation path, as well as the appearance of a weak effective nonlocality even in media with a purely Kerr (local) response.

II. MODELING LIGHT SELF-TRAPPING IN ANISOTROPIC MEDIA

We start by considering a nonmagnetic dielectric with real permittivity $\boldsymbol{\epsilon}$ in the form

$$\boldsymbol{\epsilon} = \begin{bmatrix} \epsilon_{xx} & 0 & 0 \\ 0 & \epsilon_{yy} & \epsilon_{yz} \\ 0 & \epsilon_{zy} & \epsilon_{zz} \end{bmatrix}, \tag{1}$$

with the optic axis lying in the plane yz and ϵ_{il} $(i,l = x,y,z)$ also accounting for a space-dependent polarizability. Under the previous assumptions, Maxwell's equations admit two standard independent solutions: an ordinary wave, with an electric field vector parallel to $\hat{x}$, and an extraordinary (e) wave, with an electric field in the plane yz. However, since the ordinary eigensolution can be addressed as a limiting case of the e configuration and resembles waves in isotropic media, in the following we focus on extraordinary (e) waves. For monochromatic excitation [time dependence $\exp(j\omega t)$], Maxwell's equations read

$$\nabla \times \boldsymbol{E}_e = -j\omega\mu_0 \boldsymbol{H}_e, \tag{2}$$

$$\nabla \times \boldsymbol{H}_e = j\omega(\boldsymbol{\epsilon} \cdot \boldsymbol{E}_e + \boldsymbol{P}^{\mathrm{NL}}), \tag{3}$$

with $\boldsymbol{P}^{\mathrm{NL}}$ the nonlinear polarization. To better illustrate the underlying physics, we assume that an integration can reduce the propagation problem with two transverse dimensions [(2 + 1)D] into a (1 + 1)D case; hence, we set $\partial_x = 0$. The nonzero components of the electromagnetic field are then E_{ey}, E_{ez}, and H_{ex}, governed by

$$\left(\partial_z + \frac{\epsilon_{yz}}{\epsilon_{zz}}\partial_y\right) H_{ex} = j\omega\left[\left(\epsilon_{yy} - \frac{\epsilon_{yz}^2}{\epsilon_{zz}}\right) E_{ey} - \frac{\epsilon_{yz}}{\epsilon_{zz}} P_z^{\mathrm{NL}} + P_y^{\mathrm{NL}}\right], \tag{4a}$$

$$\left(\partial_z + \frac{\epsilon_{yz}}{\epsilon_{zz}}\partial_y\right) E_{ey} = \frac{j}{\omega\epsilon_{zz}}\partial_y^2 H_{ex} + j\omega\mu_0 H_{ex} - \frac{P_z^{\mathrm{NL}}}{\epsilon_{zz}}, \tag{4b}$$

$$E_{ez} = -\frac{\epsilon_{yz}}{\epsilon_{zz}} E_{ey} + \frac{j}{\omega\epsilon_{zz}}\partial_y H_{ex} - \frac{P_z^{\mathrm{NL}}}{\epsilon_{zz}}, \tag{4c}$$

where we found E_{ez} from the z component of Eq. (3) and then substituted the computed expression [corresponding to Eq. (4c)] in the projections of Eqs. (2) and (3) along x and y, respectively. Equations (4) describe beam propagation in a uniaxial, including nonlinear effects of any size and nature, linear and nonlinear nonhomogeneities as well as nonparaxial phenomena associated with wavelength-size transverse features. Since $\hat{z}$ is arbitrary, we take it as the direction of (forward) wave propagation. E_{ey} and H_{ex} can be normalized by scaling the spatial coordinates y and z by the wavelength λ_0 in vacuum, and Eqs. (4) suffice to fully characterize the propagation of an electromagnetic wave in a nonabsorbing nonmagnetic medium. For negligible spatial variations of $\epsilon_{yz}/\epsilon_{zz}$ (the latter corresponding to $\tan\delta$, with δ

*Corresponding author: alberucc@uniroma3.it
†assanto@uniroma3.it

the walk-off of a plane e wave with wave vector $\|\hat{z}$), we can operate the transformation

$$y' = y - (\epsilon_{yz}/\epsilon_{zz})z, \tag{5a}$$

$$z' = z. \tag{5b}$$

The use of Eqs. (5) in Eqs. (4a) and (4b) provides

$$\partial^2_{z'} H_{ex} - 2\partial_{z'}(\ln n_e)\left[\partial_{z'} H_{ex} + \frac{j\omega}{\cos\delta} P_t^{\rm NL}\right] + D\partial^2_{y'} H_{ex} + k_0^2 n_e^2 H_{ex} - \frac{j\omega}{\cos\delta}\left[\partial_{z'} P_t^{\rm NL} - D\cos\delta\,\partial_{y'} P_z^{\rm NL}\right] = 0, \tag{6}$$

where $D = \frac{\epsilon_0 n_e^2}{\epsilon_{zz}}$ is the diffraction coefficient and $n_e = \sqrt{\frac{\epsilon_{yy}\epsilon_{zz} - \epsilon_{yz}^2}{\epsilon_{zz}\epsilon_0}}$ is the refractive index of e plane waves propagating along z in a homogeneous medium with a birefringent axis locally determined by the permittivity $\boldsymbol{\epsilon}$. We also introduced the directions t and s specified by unit vectors $\hat{t} = \cos\delta\,\hat{y} - \sin\delta\,\hat{z}$ and $\hat{s} = \cos\delta\,\hat{z} + \sin\delta\,\hat{y}$, respectively. In the latter reference system, the electric field components are given by

$$E_{et} = \frac{\partial_{z'} H_{ex}}{j\omega\epsilon_0 n_e^2 \cos\delta} - \frac{j\sin\delta}{\omega\epsilon_{zz}}\partial_{y'} H_{ex} - \frac{P_t^{\rm NL}}{\epsilon_0 n_e^2 \cos^2\delta} + \frac{\sin\delta}{\epsilon_{zz}} P_z^{\rm NL}, \tag{7a}$$

$$E_{es} = \frac{j\cos\delta}{\omega\epsilon_{zz}}\partial_{y'} H_{ex} - \frac{\cos\delta}{\epsilon_{zz}} P_z^{\rm NL}. \tag{7b}$$

Since the nonlinear polarization $\boldsymbol{P}^{\rm NL}$ can be expressed as a function of $\boldsymbol{E}_e$, Eqs. (7a) and (7b) are nonlinear implicit equations linking the electric field components to the magnetic field H_{ex}. Equation (6) predicts that, in the linear regime (i.e., $\boldsymbol{P}^{\rm NL} = 0$) and in the absence of an asymmetrically distributed $\boldsymbol{\epsilon}$ with respect to y', a propagating beam with a wave vector along $\hat{z}$ has a Poynting vector at an angle δ with it [36], even in the nonparaxial regime. Specifically, the complex Poynting vector $\boldsymbol{S}$ can be written as $\boldsymbol{S} \approx \frac{Z_0}{(2n_e^{(0)}\cos\delta)}|H_{ex}|^2\hat{s}$, with Z_0 the vacuum impedance and $n_e^{(0)}$ the refractive index corresponding to the peak wave vector.

III. SOLITON PROFILES

To deal with nonparaxial solitons, let us first consider a nonlinear polarization $\boldsymbol{P}^{\rm NL} = P_y^{\rm NL}\hat{y} = -f(\boldsymbol{E}_e)H_{ex}\hat{y}$, with f a real function depending on the specific nonlinearity. Setting $H_{ex} = Ae^{-jk_0 n_e^{(0)} z'}$ with $k_0 = 2\pi/\lambda_0$ and neglecting fast linear [second term in Eq. (6)] and nonlinear variations along z' [i.e., $\partial_{z'} f(\boldsymbol{E}_e)$] in the polarization of the medium, in spite of the general formulation of the problem, A is ruled by

$$-\partial^2_{z'} A + 2jk_0\left(n_e^{(0)} + cf\right)\partial_{z'} A - D\partial^2_{y'} A - k_0^2\Delta n_e^2 A = 0, \tag{8}$$

where c is the speed of light in vacuum and $\Delta n_e^2 = \Delta n_L^2 + cf$ is an *equivalent potential* acting on the beam and stemming from linear (Δn_L^2) and nonlinear effects (cf, the latter supporting self-focusing through $\boldsymbol{P}^{\rm NL}$). Hereafter, we assume the linear index to be homogeneous, leaving the study of the interaction between linear and nonlinear index wells to future work.

Equation (8) transforms into the well-known generalized nonlinear Schrödinger equation (NLSE) when the first term can be neglected and $cf \ll n_e^{(0)}$. At variance with the isotropic case, the coefficient D in Eq. (8) differs from unity because it depends on the second derivative of the permittivity with respect to the propagation angle [20,37]. For arbitrarily large anisotropy, the calculated (using a plane-wave expansion) diffraction of a Gaussian beam in a linear homogeneous uniaxial is in perfect agreement with the theoretical result from Eq. (8). Given the ansatz for $\boldsymbol{P}^{\rm NL}$, in this case the nonlinearity does not affect the walk-off (i.e., the soliton trajectory). We consider a generic third-order nonlinear and nonlocal dielectric with the response [38,39]

$$\Delta n_e^2 = \int_{-\infty}^{\infty} [G_{yy}(y'-\xi)|E_{ey}|^2 + G_{zz}(y'-\xi)|E_{ez}|^2 + 2G_{yz}(y'-\xi)\mathrm{Re}(E_{ey}E_{ez}^*)]d\xi. \tag{9}$$

For the sake of clarity we simply set $G_{yy} = G_{zz} = G_{yz} = n_2 G$, with n_2 proportional to the Kerr coefficient and $\int G(y')dy' = 1$. Various sizes of nonlocality are accounted for through parameter w in the Gaussian $G(y') = 1/\sqrt{\pi w^2}e^{-y'^2/w^2}$. We look for self-trapped waves in the form of spatial solitons

$$A(y',z') = u(y')e^{-jk_0 n_{\rm NL} z'}, \tag{10}$$

with u the magnetic field profile and $n_{\rm NL}k_0$ the nonlinear contribution to the propagation constant. We stress that the position made in Eq. (10) corresponds to considering solitons which propagate at an angle δ (i.e., the linear walk-off) with $\hat{z}$ in the laboratory frame yz. From Eq. (8) it is straightforward to get the eigenvalue problem

$$\left(n_{\rm NL}^2 + 2n_{\rm NL}n_e^{(0)}\right)k_0^2 u = D\partial^2_{y'} u + k_0^2\Delta n_e^2 u, \tag{11}$$

where Δn_e^2 depends on the beam power through Eq. (9) and the electric field components are those in Eqs. (4). From Eqs. (9)–(11) we find that u is a real function, hence the Poynting vector is

$$\boldsymbol{S} = \frac{Z_0\left(n_e^{(0)} + n_{\rm NL}\right)}{2n_e^2\cos\delta}|u|^2\hat{s} + \frac{j}{2\omega\epsilon_{zz}}u\partial_{y'}u\;\hat{y}. \tag{12}$$

We start discussing the highly nonlocal case where the nonlinear perturbation of the permittivity well (index of refraction) is much wider than the beam waist. In this limit an analytic solution can be found for solitons [7]. Neglecting terms proportional to $|\partial_{y'}u|^2$, Eq. (9) becomes $\Delta n_e^2 = n_2\int G^{\rm tot}|u|^2dy'$, with $G^{\rm tot} = Z_0^2(\frac{n_e^{(0)}+n_{\rm NL}}{n_e^2})^2(\tan\delta - 1)^2 G$. After defining the normalized Kerr coefficient $n_{2H} = n_2 Z_0\cos\delta(\tan\delta-1)^2/n_e^{\max}$ ($n_e^{\max}$ is the peak of n_e with respect to y'), we introduce the beam width $\sigma = \sqrt{\int y'^2|H_{ex}|^2dy'/\int|H_{ex}|^2dy'}$, the power per unit-wavefront P_d (Wm^{-1}), and the n derivative G_n of Green's function $G(y')$ evaluated in $y' = 0$, and obtain $\Delta n_e^2 \approx (G_0 + 0.5G_2\sigma^2)n_{2H}P_d + n_{2H}G_2P_d y'^2$ [40]. For a Gaussian Green's function $\Delta n_e^2 = \frac{1}{w\sqrt{\pi}}(1 - \frac{w_A^2}{2w^2})n_{2H}P_d - \frac{n_{2H}P_d}{w^3\sqrt{\pi}}y'^2$, with w_A the waist of a soliton $A = (\frac{2n_e^{\max}\cos\delta}{Z_0\sqrt{\pi}}\frac{P_d}{w_A})^{\frac{1}{2}}e^{-y'^2/w_A^2}e^{-jn_{\rm NL}k_0 z'}$. If $n_{\rm NL} \ll n_e^{(0)}$ (i.e., at low powers), the nonlinear propagation constant is fixed by $n_{\rm NL}k_0 = \frac{1}{w\sqrt{\pi}}(1 - \frac{w_A^2}{2w^2})n_{2H}P_d k_0 - n_e^{(0)}\sqrt{\frac{Dn_{2H}P_d}{n_e^{\max}w^3\sqrt{\pi}}}$, where the term linear in P_d is the increase

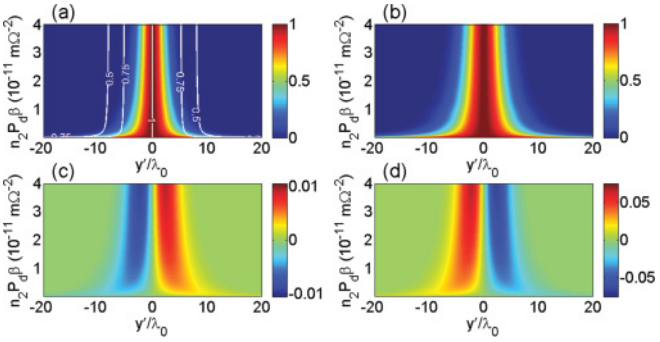

FIG. 1. (Color online) Soliton profiles for $w/\lambda_0 = 9.4$ and $\delta = 8^\circ$. (a) Square modulus of the magnetic field H_{ex} and index well Δn_e^2 (contour plot) vs y'/λ_0 and effective excitation $n_2 P_d \beta$, with $\beta = 2n_e^{(0)} \cos\delta / Z_0$; the quantities are normalized to their peak values for each $n_2 P_d \beta$ in order to compare the relative width. (b) Real part of E_{et} vs y'/λ_0 and $n_2 P_d \beta$. (c)–(d) As in (b) but for the imaginary part of E_{et} and E_{es}, respectively. The quantities in (b)–(d) are normalized to the modulus of the maximum E_{et} for each $n_2 P_d \beta$.

of the maximum index and the other relates to the convexity of the self-induced parabolic well. We stress that whenever the nonlinearity is Kerr like (i.e., the change in index is linear with intensity), the *effective action* of the nonlinear perturbation depends on the product $n_{2H} P_d$.

Figure 1 plots numerically computed soliton solutions of the nonlinear eigenvalue problem consisting of Eqs. (7) and (9)–(11), and accounting for $\partial_{y'} u$ in Eq. (9): u and $\mathrm{Re}(E_{et})$ are bell-shaped [Figs. 1(a) and 1(b)], whereas $\mathrm{Im}(E_{et})$ (much smaller than the real part) and $E_{es} = j\mathrm{Im}(E_{es})$ (purely imaginary) have an odd symmetry since they are proportional to $\partial_{y'} u$ [Figs. 1(c) and 1(d)]; hence, their amplitudes grow as the beam width σ reduces, with an increasing degree of profile asymmetry, as shown in the plot of *transversality*, i.e., the ratio $\max(|E_{et}|)/\max(|E_{es}|)$, in Fig. 2(a). Moreover, narrower solitons (lower transversalities) correspond to higher powers, as visible in Fig. 2(b). The soliton waist $w_A = 2\sigma$ at high power tends to 0.5, consistent with the diffraction limit of a focused beam. For a fixed excitation, the beam waist increases for higher ratios w/λ_0 owing to a lower Δn_e^2, consistent with

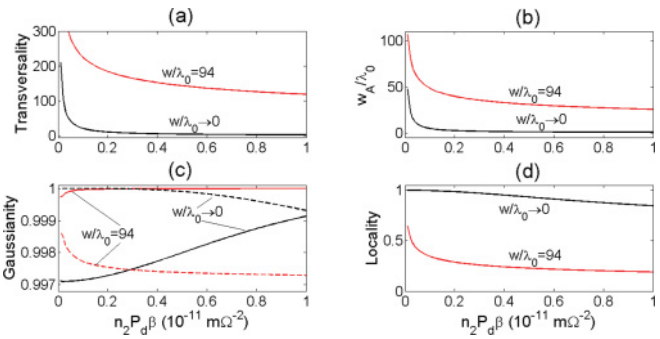

FIG. 2. (Color online) Main features of anisotropic solitons vs excitation $n_2 P_d \beta$ for various w/λ_0. (a) Ratio between maxima of $|E_{et}|$ and $|E_{es}|$; (b) normalized soliton waist w_A/λ_0; (c) scalar product of soliton and best Gaussian (solid lines) or sech (dotted lines) fitting functions; (d) figure of locality, i.e., ratio between the widths of the soliton u and of the index well. Here $\delta = 8^\circ$ and $n_e^{(0)} = 1.6$.

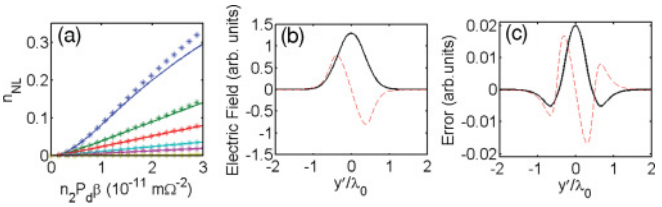

FIG. 3. (Color online) (a) Effective nonlinear index n_{NL} vs excitation $n_2 P_d \beta$ for various ratios w/λ_0 (increasing downward), computed by neglecting (dots) or including (solid lines) the second derivative along z'. The top line is the local case; the others from top to bottom correspond to $w/\lambda_0 = 0.94, 1.9, 4.7, 9.4, 94.0$, respectively. (b) Soliton profile calculated in the local case from the complete model with $n_2 P_d \beta = 3 \times 10^{-11} \mathrm{m}\Omega^{-2}$ and (c) corresponding error in soliton profile when neglecting $\partial_z^2 u$ in the model. Black solid and red dashed lines in (b) and (c) are $\mathrm{Re}(E_t)$ and $\mathrm{Im}(E_s)$, respectively.

the highly nonlocal limit. For a fixed w/λ_0, Fig. 2(c) shows how the soliton adjusts from sech to Gaussian profiles as the power increases (and w_A diminishes): the system evolves from local to nonlocal with excitation [see Figs. 1(a) and 2(d)]. One of the most remarkable effects of the pronounced asymmetry (Fig. 1) is that, in the nonparaxial limit, even purely Kerr media become moderately nonlocal since Δn_e^2 depends on $\partial_{y'} u$ through Eq. (9). Since walk-off primarily affects the relationship between $E_{et/es}$ and $E_{ey/ez}$, these results bear a slight dependence on δ (see the definition of n_{2H}) but also apply to isotropic media (and ordinary waves) where $\delta = 0$. Figure 3(a) shows the calculated n_{NL} versus excitation $n_2 P_d \beta$ for various w/λ_0 when $\partial_{z'}^2 u$ is either included (dots) or neglected (solid lines): the difference between the two cases is appreciable for $n_{\mathrm{NL}} > 0.2$. Figures 3(b) and 3(c) illustrate and compare the corresponding soliton profiles.

IV. SELF-STEERING VIA NONLINEAR WALK-OFF IN PURELY KERR MEDIA

Aiming at generalizing the above analysis of nonparaxial soliton physics, we now address the role of each nonlinear term in Eq. (6) for anisotropic (uniaxial) media with a Kerr (local) nonlinearity $\boldsymbol{P}^{\mathrm{NL}} = \Phi \boldsymbol{E}_e$ with, e.g., $\Phi = \epsilon_0 n_2 (|E_{es}|^2 + |E_{et}|^2)$, i.e., a non-negligible $\partial_{y'} P_z^{\mathrm{NL}}$ in Eq. (6). We find solitons in the form given by Eq. (10), thus fixing the direction of energy propagation.

For a generic nonlinear polarization in the form $\boldsymbol{P}_{\mathrm{NL}} = \boldsymbol{p}_{\mathrm{NL}} e^{-jk_0(n_e^{(0)} + n_{\mathrm{NL}})}$ and starting from Eq. (8), Eq. (11) becomes

$$-k_0^2 \left(n_{\mathrm{NL}}^2 + 2n_e^{(0)} n_{\mathrm{NL}}\right) u + D\partial_{y'}^2 u - \frac{k_0^2 c \left(n_e^{(0)} + n_{\mathrm{NL}}\right)}{\cos\delta} p_t^{\mathrm{NL}} + jk_0 c D \partial_{y'} p_z^{\mathrm{NL}} = 0, \quad (13)$$

where we supposed the absence of a linear index well. The Poynting vector can be cast as

$$\boldsymbol{S} = \frac{1}{2}\left[\hat{s}\left(\frac{n_e^{(0)} + n_{\mathrm{NL}}}{n_e^2 \cos\delta} Z_0 |u|^2 + \frac{j \sin\delta}{\omega \epsilon_{zz}} u^* \partial_{y'} u + \frac{p_t^{\mathrm{NL}} u^*}{\epsilon_0 n_e^2 \cos\delta} - \frac{\sin(\delta) p_z^{\mathrm{NL}} u^*}{\epsilon_{zz}}\right) + \hat{t}\left(\frac{j \cos\delta}{\omega \epsilon_{zz}} u^* \partial_{y'} u - \frac{\cos\delta}{\epsilon_{zz}} u^* p_z^{\mathrm{NL}}\right)\right]. \quad (14)$$

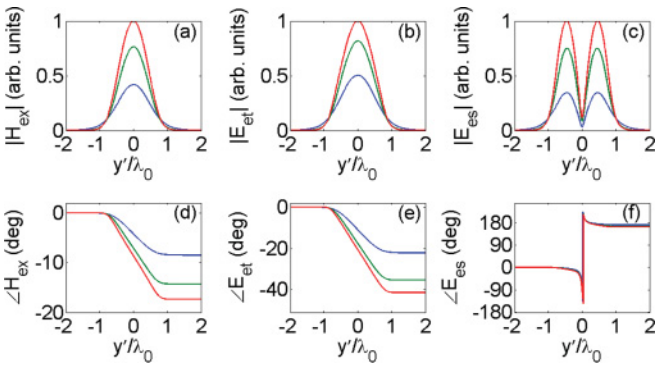

FIG. 4. (Color online) Self-steering solitons. Calculated modulus of (a) magnetic field, (b) tangential, and (c) longitudinal electric field vs y'/λ_0. Blue, green, and red lines (from bottom to top) correspond to $n_2 P_d \beta = (1,3,5) \times 10^{-11}$ mΩ^{-2}, respectively. (d)–(f) Corresponding phase profiles vs y'/λ_0; the transverse phase jump increases with excitation. Here $\delta = 8^\circ$.

The factor proportional to $p_t^{\rm NL}$ in Eq. (13) reduces to a nonlinear index variation of the form $\Delta n_e^2 \propto \Phi$; hence, the results previously obtained from Eq. (8) hold valid. In Eqs. (7a)-(7b), we neglect terms depending on $p_z^{\rm NL}$ (lower than $p_t^{\rm NL}$ for realistic nonlinearities), being the nonlinear polarization much smaller than the linear one in the local case (see Fig. 3). Setting $k_t = -Z_0(n_{\rm NL} + n_e^{(0)})(n_e^2 \cos\delta)$ and $k_s = \cos\delta/(\omega\epsilon_{zz})$, we can write $j\omega D\partial_{y'} p_z^{\rm NL} = \omega D[k_s \cos\delta(\partial_{y'}\Phi\partial_{y'}u + \Phi\partial_{y'}^2 u) - jk_t \sin\delta(\Phi\partial_{y'}u + u\partial_{y'}\Phi)]$, where the imaginary part of E_{et} is neglected in line with the results of Fig. 1(c). The real terms (multiplied by k_s) are even and affect the profile of the nonlinear index well, as well as of the soliton; the imaginary terms (multiplied by k_t) distort the soliton phase front; hence, they modify the soliton path. Figure 4 shows numerical computations of the electromagnetic field of a soliton with the Poynting vector fixed along z', i.e., at angle δ with z in the plane yz, demonstrating the appearance of a self-induced tilt in the beam phase front owing to a nonlinear variation in walk-off with excitation. Let us now focus on the Poynting vector given by Eq. (14): $p_z^{\rm NL}$ is neglected, consistent with the approximation made in calculating the soliton profile, whereas $p_t^{\rm NL}$ gives rise to a y'-dependent change (proportional to Δn_e^2) in the amplitude of the s component of the Poynting vector. Finally, the two last terms containing $u^*\partial_{y'}u$ can be grouped as $j/(\omega\epsilon_{zz})\hat{y}u^*\partial_{y'}u$. Writing u in polar form, we get $u^*\partial_{y'}u = |u|\partial_{y'}|u| + j|u|^2\partial_{y'}(\angle u)$; hence, the real part of $\boldsymbol{S}$ along $\hat{y}$ is proportional to $|u|^2\partial_{y'}(\angle u)$ and even with respect to y'. Thus, we have a nonzero (transverse) transfer of real energy across the soliton profile. Eventually, we remark that this kind of light self-steering effect does not occur in isotropic media where $\delta = 0$.

V. HIGHLY NONPERTURBATIVE REGIME: REORIENTATIONAL CASE

In the previous sections we neglected the nonlinear polarization term $\boldsymbol{P}_{\rm NL}$ in Eqs. (7), which is a good approximation for a large variety of materials and excitation conditions (see Fig. 3). In this section we will focus on a specific system where the latter approximation does not hold valid for large enough powers, namely, nematic liquid crystals (NLCs). NLCs are known to exhibit very high effective nonlinearities (typically $n_2 \approx 10^{-6}$ cm^2 W^{-1}) due to the particular nature of light-matter interactions [41–43]. Consequently, in uniaxial NLCs, the optic axis (or molecular *director*) can reorientate in space by reacting to low electric fields, i.e., light beams of powers in the milliwatt or even microwatt range [44,45]: when the induced rotation becomes comparable with the initial distribution, the nonlinear polarization is no longer negligible with respect to the linear one. Light self-steering owing to nonlinear changes in walk-off was experimentally demonstrated in the modulational instability regime [46,47] and for stable self-trapped beam propagation [48].

With reference to light self-trapping, NLCs behave as a saturable nonlocal nonlinear medium able to support stable $(2+1)$D spatial solitons at relatively low cw excitations [11,44,48,49]. At low powers, the soliton trajectories do not bend because of the negligible walk-off variations associated with the optically induced reorientation [11]; at higher powers, beam self-bending can be expected [48,49]. We refer to a planar NLC cell, infinitely extended along y and z and with a finite thickness L across x [11]. The boundary conditions induce a homogeneous director distribution in the absence of excitation, with the optic axis lying in the plane yz at an angle θ_0 with respect to z. Equations (4) need be solved in conjunction with those ruling the director distribution [11,41,43]; since the electric field vector belongs to the plane yz, the director remains coplanar at an angle θ with respect to axis z; θ is governed by [11]

$$K\nabla^2\theta + \epsilon_a[\sin(2\theta)(|E_{ey}|^2 - |E_{ez}|^2) + 2{\rm Re}(E_{ey}E_{ez}^*)\cos(2\theta)] = 0, \quad (15)$$

with K the Frank elastic constant (for molecular deformations) and ϵ_a the dielectric anisotropy. We look for single-hump solitary solutions having a flat-phase transverse profile, i.e., in the form $H_{ex} = u(y')e^{-j(n_e^{(0)}+n_{\rm NL})k_0 z}$ with u real and $\theta = \theta_u(y')$, where we set $y' = y - z\tan\delta$ and where δ is the power-dependent walk-off. Therefore, we fix the wave vector and allow the Poynting vector to change its direction in yz, in agreement with typical experimental setups [11,48]. Due to the high nonlocality of this medium [8,11], to compute the soliton profile we can use Eq. (8), taking for δ and $n_e^{(0)}$ the value computed at the beam peak (solitons are even due to symmetry). In other words, following the approach of self-consistent soliton theory [50] and assuming $\theta_u - \theta_0$ known, we can consider the latter as a *linear* inhomogeneous distribution of the optic axis, and keep into account that the nonlinear perturbations on θ *effectively* are perceived by the soliton (i.e., through spatial overlap with its intensity profile) as small because of the high nonlocality; hence, only transverse variations in the refractive index n_e are relevant.

To get a simplified $(1+1)$D model for nonlinear optical propagation, in Eq. (15) we make the ansatz $\sin(\pi x/L)$ (the cell boundaries are in $x = 0, L$) for the x dependence of the optical perturbation $\theta_u - \theta_0$ and consider beams propagating in the cell midplane $x = L/2$ [49]. Therefore, we have to solve

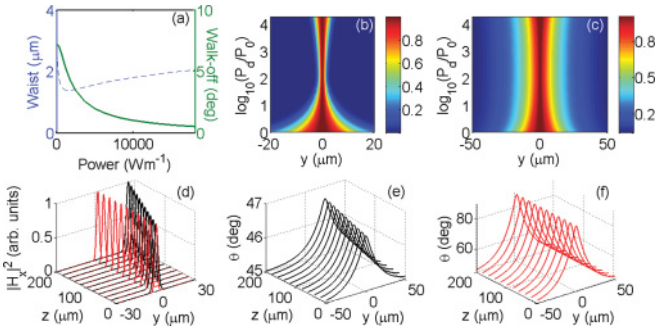

FIG. 5. (Color online) Soliton self-steering in NLC. (a) Soliton waist (dashed blue line) and walk-off (solid green line) vs power density. (b) Plots of $|H_x|$ and the optical perturbation $\theta - \theta_0$ in the soliton case, vs y and the logarithm of the power density P_d, with $P_0 = 62$ Wm^{-1}. Both quantities are normalized to their peak value at each power. (d) Beam evolution in yz computed by the BPM (beam propagation method) when the input profile corresponds to a solitary solution for $P_d = 62$ Wm^{-1} (black lines, beam with the largest slope in yz) and $P_d = 1.8 \times 10^4$ Wm^{-1} (red lines). (e) and (f) show the corresponding perturbation in the director distribution in the cell. In this example, $\lambda_0 = 442$ nm, $n_\perp = 1.5$, $n_\parallel = 1.7$, $K \approx 10^{-11}$N, $\theta_0 = \pi/4$, and $L = 50$ μm.

the $(1+1)$D nonlinear eigenvalue problem

$$\left(2n_{\rm NL}n_e^{(0)} + n_{\rm NL}^2\right)k_0^2 u = D\partial_{y'}^2 u + k_0^2 \Delta n_e^2 u, \qquad (16a)$$

$$(1+\tan^2\delta)\partial_{y'}^2\theta_u - \left(\frac{\pi}{L}\right)^2(\theta_u - \theta_0) + \epsilon_a[\sin(2\theta_u)(|E_{ey}|^2 - |E_{ez}|^2) + 2\cos(2\theta_u)\mathrm{Re}(E_{ey}E_{ez}^*)] = 0. \qquad (16b)$$

Figure 5 shows numerical solutions of system of Eqs. (16) for $\theta_0 = \pi/4$: due to the reorientational nonlinearity, the induced optical perturbation saturates at high power, resulting in a nonmonotonic trend for the soliton waist with power [Fig. 5(a)]. Figure 5(a) graphs also the walk-off δ versus power, demonstrating soliton self-bending. Figures 5(c) and 5(d) plot the profiles of u and θ_u versus y' and power density P_d: u is very close to Gaussian due to the NLC high nonlocality, whereas the optical perturbation $\theta_u - \theta_0$ is very similar to Green's function of the structure with a width slightly changing versus power, exponentially decreasing for large $|y'|$ with a slope determined by L [49].

Using a BPM propagator with a relaxation algorithm to calculate the director distribution in yz, we checked that the calculated solutions effectively correspond to solitons by simulating their propagation in an NLC cell with Eq. (8) (where $\partial_{z'}^2 A$ is neglected) together with the reorientation equation in the plane $x = L/2$, respectively. It is noteworthy that the second derivative contribution in Eq. (8) is vanishing because we take for $n_e^{(0)}$ the refractive index at the maximum reorientation. As shown in Fig. 5(d), the beams walk-off with invariant profiles, confirming the validity of the computed solutions and the occurrence of power-dependent angular self-steering. The corresponding optically perturbed director distributions are visible in Figs. 5(e) and 5(f).

VI. SELF-STEERING IN NONCENTROSYMMETRIC MEDIA

Finally, we consider a linearly isotropic medium (i.e., $\delta = 0$) with a Kerr response lacking inversion symmetry; in this case, the z component of the nonlinear polarization in general contains a term proportional to ΦE_y with $\Phi \propto (|E_z|^2 + \gamma|E_y|^2)$ and γ a constant related to the cubic susceptibility tensor $\chi^{(3)}$. Neglecting extra contributions to $P_z^{\rm NL}$, $\partial_{y'}P_z^{\rm NL} = k_t(u\partial_{y'}\Phi + \Phi\partial_{y'}u)$ yields an odd (imaginary) term in Eq. (6). Therefore, similar to what was discussed above, a noncentrosymmetric nonlinear response breaks the parity and provides nonlinear steering of the soliton trajectory depending on the transverse gradient of the longitudinal nonlinear polarization.

VII. CONCLUSIONS

In conclusion, we have derived a model governing nonlinear propagation of electromagnetic beams in inhomogeneous uniaxials, taking into account the longitudinal field component arising in the nonparaxial regime. Our model and calculations demonstrate that, regardless the degree of nonlocality or despite it, nonparaxiality introduces asymmetry in soliton transverse profiles and a weak nonlocality, even in the case of purely Kerr media. We demonstrated self-steering effects due to nonlinear walk-off changes in the presence of strong self-confinement in Kerr media with an anisotropic linear behavior. In the highly perturbative regime, we demonstrated how such effect can take place even though the longitudinal electric field remains negligible with respect to the transverse one, referring to NLC as a realistic example. In noncentrosymmetric media and in the nonparaxial regime we predicted that asymmetry in the longitudinal field can lead to self-action of the light beam on its own trajectory.

With reference to applications, light self-steering can play an important role in the design and realization of optical networks with topology controlled by the signal itself. Our results have also potential implications in particle confinement and manipulation via tightly focused light beams. Finally, we expect these findings to have an impact on self-confinement of longitudinal waves in diverse fields such as acoustics, fluid dynamics, and atom optics.

ACKNOWLEDGMENTS

We thank A. Piccardi for fruitful discussions. This effort is partially sponsored by the Air Force Office of Scientific Research, Air Force Material Command, USAF, under Grant No. FA-8655-10-1-3010. The US government is authorized to reproduce and distribute reprints for Governmental purpose notwithstanding any copyright notation thereon.

[1] P. G. Drazin and R. S. Johnson, *Solitons: an Introduction* (Cambridge University Press, Cambridge, England, 1993).

[2] T. Dauxois and M. Peyrard, *Physics of Solitons* (Cambridge University Press, Cambridge, England, 2006).

[3] Y. S. Kivshar and G. P. Agrawal, *Optical Solitons* (Academic, San Diego, CA, 2003).
[4] H.-Y. Hao and H. J. Maris, Phys. Rev. B **64**, 064302 (2001).
[5] C. Conti, G. Ruocco, and S. Trillo, Phys. Rev. Lett. **95**, 183902 (2005).
[6] C. Conti and G. Assanto, in *Encyclopedia of Modern Optics* (Elsevier, Oxford, 2004), Vol. 5, p. 43.
[7] A. W. Snyder and D. J. Mitchell, Science **276**, 1538 (1997).
[8] C. Conti, M. Peccianti, and G. Assanto, Phys. Rev. Lett. **91**, 073901 (2003).
[9] C. Conti, M. Peccianti, and G. Assanto, Phys. Rev. Lett. **92**, 113902 (2004).
[10] C. Rotschild, O. Cohen, O. Manela, M. Segev, and T. Carmon, Phys. Rev. Lett. **95**, 213904 (2005).
[11] M. Peccianti, C. Conti, G. Assanto, A. DeLuca, and C. Umeton, Nature (London) **432**, 733 (2004).
[12] G. Assanto, Z. Wang, D. J. Hagan, and E. W. Van Stryland, Appl. Phys. Lett. **67**, 2120 (1995).
[13] J. U. Kang, G. I. Stegeman, J. S. Aitchison, and N. Akhmediev, Phys. Rev. Lett. **76**, 3699 (1996).
[14] W. E. Torruellas, G. Assanto, B. L. Lawrence, R. A. Fuerst, and G. I. Stegeman, Appl. Phys. Lett. **68**, 1449 (1996).
[15] L. Torner, D. Mihalache, D. Mazilu, and N. Akhmediev, Opt. Comm. **138**, 105 (1997).
[16] T. G. Canva, R. A. Fuerst, S. Baboiu, G. I. Stegeman, and G. Assanto, Opt. Lett. **22**, 1683 (1997).
[17] G. Leo, G. Assanto, and W. E. Torruellas, Opt. Lett. **22**, 7 (1997).
[18] L. Bergé, O. Bang, and W. Krolikowski, Phys. Rev. Lett. **84**, 3302 (2000).
[19] G. Assanto and G. Stegeman, Opt. Express **10**, 388 (2002) [http://www.opticsinfobase.org/oe/abstract.cfm?URI=oe-10-9-388].
[20] C. Conti, M. Peccianti, and G. Assanto, Phys. Rev. E **72**, 066614 (2005).
[21] A. Piccardi, A. Alberucci, and G. Assanto, Phys. Rev. Lett. **104**, 213904 (2010).
[22] M. Lax, W. H. Louisell, and W. B. McKnight, Phys. Rev. A **11**, 1365 (1975).
[23] S. Chi and Q. Guo, Opt. Lett. **20**, 1598 (1995).
[24] B. Crosignani, P. D. Porto, and A. Yariv, Opt. Lett. **22**, 778 (1997).
[25] P. Chamorro-Posada, G. McDonald, and G. New, J. Mod. Optic. **45**, 1111 (1998).
[26] S. Blair, Chaos **10**, 570 (2000).
[27] A. Ciattoni, C. Conti, E. DelRe, P. DiPorto, B. Crosignani, and A. Yariv, Opt. Lett. **27**, 734 (2002).
[28] G. Baruch, G. Fibich, and S. Tsynkov, Opt. Express **16**, 13323 (2008).
[29] A. Ciattoni, B. Crosignani, P. DiPorto, and A. Yariv, Phys. Rev. Lett. **94**, 073902 (2005).
[30] Y. Liu, G. Bartal, D. A. Genov, and X. Zhang, Phys. Rev. Lett. **99**, 153901 (2007).
[31] A. R. Davoyan, I. V. Shadrivov, A. A. Zharov, D. K. Gramotnev, and Y. S. Kivshar, Phys. Rev. Lett. **105**, 116804 (2010).
[32] F. Ye, D. Mihalache, B. Hu, and N. C. Panoiu, Phys. Rev. Lett. **104**, 106802 (2010).
[33] R. Dorn, S. Quabis, and G. Leuchs, Phys. Rev. Lett. **91**, 233901 (2003).
[34] V. G. Shvedov, A. V. Rode, Y. V. Izdebskaya, A. S. Desyatnikov, W. Krolikowski, and Y. S. Kivshar, Phys. Rev. Lett. **105**, 118103 (2010).
[35] S. V. Afshar and T. M. Monro, Opt. Express **17**, 2298 (2009).
[36] D. Bhawalkar, A. Goncharenko, and R. Smith, Br. J. Appl. Phys. **18**, 1431 (1967).
[37] M. Nazarathy and J. Goodman, J. Opt. Soc. Am. A **3**, 523 (1986).
[38] R. W. Boyd, *Nonlinear Optics* (Academic, Boston, 1992).
[39] W. Krolikowski and O. Bang, Phys. Rev. E **63**, 016610 (2000).
[40] Q. Guo, B. Luo, F. Yi, S. Chi, and Y. Xie, Phys. Rev. E **69**, 016602 (2004).
[41] N. Tabiryan and B. Zeldovich, Mol. Cryst. Liq. Cryst. **62**, 237 (1980).
[42] F. Simoni, *Nonlinear Optical Properties of Liquid Crystals* (World Scientific, Singapore, 1997).
[43] I. C. Khoo, Phys. Rep. **471**, 221 (2009).
[44] S. V. Serak, N. V. Tabiryan, M. Peccianti, and G. Assanto, IEEE Photon. Techn. Lett. **18**, 1287 (2006).
[45] A. Piccardi, A. Alberucci, and G. Assanto, Electron. Lett. **46**, 790 (2010).
[46] M. Peccianti, C. Conti, and G. Assanto, Phys. Rev. E **68**, 025602(R) (2003).
[47] M. Peccianti and G. Assanto, Opt. Lett. **30**, 2290 (2005).
[48] A. Piccardi, A. Alberucci, and G. Assanto, Appl. Phys. Lett. **96**, 061105 (2010).
[49] A. Alberucci and G. Assanto, Opt. Lett. **35**, 2520 (2010).
[50] A. W. Snyder, D. J. Mitchell, L. Poladian, and F. Ladouceur, Opt. Lett. **16**, 21 (1991).